https://doi.org/10.1109/ICRA40945.2020.9197577

Exploration of 3D terrains using potential fields with elevation-based local distortions

Renan Maffei[1] Marcos P. Souza[1] Mathias Mantelli[1] Diego Pittol[1] Mariana Kolberg[1] Vitor A. M. Jorge[2]

***Abstract*— Mobile robots can be used in numerous outdoor tasks such as patrolling, delivery and military applications. In order to deploy mobile robots in this kind of environment, where there are different challenges like slopes, elevations, or even holes, they should be able to detect such challenges and determine the best path to accomplish their tasks. In this paper, we are proposing an exploration approach based on potential fields with local distortions, in which we define preferences in uneven terrains to avoid high declivity regions without compromising the best path. The approach was implemented and tested in simulated environments, considering a ground robot embedded with two 2D LIDAR sensors, and the experiments demonstrated the efficiency of our method.**

I. Introduction

Autonomous exploration is fundamental for mobile robots operating autonomously in unknown or partially unknown environments. Over the years, several exploration approaches [1], including planners involving potential fields [2]–[5], have been devised for structured planar indoor environments.

Recently, the focus started to move from structured indoor environments to unstructured outdoor environments with uneven terrain [6], which broadens the applications of autonomous robots, but also adding increased traversability problems. Uneven terrains may, or may not, be accessible to an autonomous robot depending on terrain declivity, i.e., the separation between obstacles and free regions is less clear to detect. Unstructured and uneven environments may pose kinematic constraints to the robot (e.g., region is too steep), or add increased or decreased energy expenditure [7] depending on terrain declivity. Therefore, terrain classification and the definition of actions for each terrain type [7]–[13], become fundamental problems for autonomous exploration.

In the area of potential fields, while some approaches are now focusing on uneven terrain [13], [14], most of them keep the traditional focus on indoor and structured environments [2], [5], [15]. Still, the application of potential fields to the exploration problem is quite interesting. For instance, Prestes et al. [15] developed an exploration strategy relying on the Boundary-Value Problem (BVP) resolving the Laplace equation. The potential update algorithm is made with a relaxation method, such as Gauss-Seidel, that solves the problem incrementally and allows the use of partial solutions. For that, we just need to define correctly the boundary conditions (obstacles and goals, which in the mapping problem correspond to unexplored areas), which is simple when we have a grid map. Nevertheless, arguably the main advantage of the BVP exploration is that the potential field generated from the Laplace equation is a harmonic function, free of local minima, which is one of the main weaknesses of other potential field approaches. This means that after computing the potential field we can always find a path from any position in the map to the goal, and the path is safe, i.e., far from obstacles, and smooth, which is specially suitable for robot control. On the other hand, one of the main problems of the BVP strategy is the high computational cost involved for computing the potential field, which, for example, greatly hinders its use in 3D environments.

Over the last years, extensions were presented for the BVP exploration, mainly focusing on improving computation speed, such as the use of local windows [16] and multigrid strategies [17]. Another major point of research is the generation of local distortions in the potential field, that modifies the robot path during exploration to consider regions with different preferences [4], [18]. However, even though potential distortions have the possibility of being used in uneven terrains, research in this area is still open.

Our proposal is an exploration strategy based on BVP for uneven 3D terrains, that is computed over a 2D grid associated to an elevation map, which is crucial to circumvent the high costs associated with the potential field update. The proposed strategy takes advantage of potential distortions to define preferences in environments with varying declivity, including regions where the autonomous robot cannot traverse, e.g., trees, stones, and so on. The proposed algorithm is able to avoid high declivity regions without completely blocking access to them. This is particularly important when the robot has to cover such terrain and a complete obstruction may lead to failure to accomplish the mission. Another feature of the algorithm is to provide a global potential distortion parameter used to avoid potential flattening, a known limitation of BVP planners. In addition to that, the algorithm proposes a mechanism to constrain the influence of potential distortions, avoiding convergence problems. The resulting

[1]Institute of Informatics, Universidade Federal do Rio Grande do Sul, Porto Alegre, Brazil rqmaffei, marcos.souza, mathias.fassini, dpittol, mariana.kolberg@inf.ufrgs.br

[2]Instituto Tecnológico de Aeronáutica, Electronic Enginnering Division, Sao Jose dos Campos, Brazil vitormj@ita.br

This study was financed in part by the Brazilian National Council for Scientific and Technological Development (CNPq) and by the Coordenação de Aperfeiçoamento de Pessoal de Nível Superior - Brasil (CAPES) - Finance Code 001.

algorithm relies on a single partial differential equation to attain a smooth trajectory toward the goal, avoiding steep regions when required, ideal for outdoor environments or indoor environments where the robot faces uneven terrain. The algorithm is tested in simulation environments using Gazebo and ROS.

This paper is presented as follows. Section II presents relevant work on autonomous exploration in uneven environments. Sections III and IV present the proposed approach and experimental results. Section V presents conclusion and future work.

II. Related Work

There are different approaches related to the problem of exploring unstructured uneven terrains and traversability problems. A recent survey on traversability problems focusing on Unmanned Ground Vehicles (UGVs) is presented by Papadakis [6]. In the seminal work of Kweon and Kanade [8], a digital elevation map is constructed using a range of 3D vision-based sensors to construct a digital elevation map of rugged terrains and using them to correct localization errors. Joho et al. [19] trades off the expected information gain and the cost of executing an action to construct 3D maps. Steep slope regions are detected and avoided to protect the robot by analyzing gaps in the sensor readings. Kuthirummal et al. [9] uses LIDARs and stereo sensors to robustly obtain elevation maps as 2D grid-cells from point clouds and create a graph portraying safe regions which the robot can traverse. Santamaria et al. [11] present two methods based on Gaussian processes: one online technique using time-of-flight camera to detect obstacles and holes; and an offline technique using laser range finders to learn traversable regions. Martin and Corke [7] are concerned with energy expenditures as a function of terrain traversability, which are used to explore and construct maps focusing on minimum energy. Suger et al. [10] points out security issues for the robot involving traversability constraints. They present a way for different robots to learn their traversability capabilities from human operators. Despite not being a UGV, Shen et al. [14] devise an efficient algorithm employing system of particles governed by a stochastic differential equation to perform autonomous 3D exploration using a micro-aerial vehicles (MAVs). Bircher et al, [20] devise a path planning algorithm for outdoor environments using MAVs, based on a receding horizon approach, using a geometric random tree to sample upcoming configurations.

Concerning potential fields methods, relevant for the present work, there are approaches which handle unstructured uneven terrain while traversing it. Vlantis et al. [21] addressed the problem of robot motion planning in a static and bounded environment with arbitrary connectedness and shape. Their proposal is based on harmonic potential fields and appropriate adaptive laws that can safely navigate a robot to its goal state from almost all initial configurations. Munoz et al. [22] also presented a work related to robot navigation, in which the robot trajectories are generated using Artificial Potential Fields and the sensed depth information from the environment. They used polar control laws to move the robot, that can reach a goal and continuously replaning its path without collisions. In addition to the potential fields, Friudenberg and Koziol [23] are also using Parallel Navigation (PN) to propose a navigation method with obstacles avoidance. Their proposed combined algorithm is able to guide the robot to rendezvous with a moving target while avoiding obstacles in its path. Another combination of potential field and other methods was introduced by Chen et al. [24]. They combined point cloud semantic segmentation with potential field in order to propose a robust navigation method for mobile robots in unknown indoor environments. Rodrigues et al. [13] use low-level visual information to construct a potential information field in uneven terrains to improve localization of a mobile robot and drive it toward the goal, by associating image features with reactive or attractive potentials and without the need of constructing a map.

Finally, our proposal is based on a specific type of potential fields, the ones involving the solution of a Boundary-Value Problem (BVP) [3], [4], [15]. Prestes et al. [15] presented the BVP-based exploration that solves the Laplace equation with Dirichlet boundary conditions over a 2D grid map. The method was improved [16] by using a local window with size varying according to the smallest sonar reading. Vallve and Cetto [2] used the entropy of the map with traditional frontier-based exploration to create a gradient of the potential information field, where the quality of the map, loop-closures and coverage are considered. Silveira et al. [17] proposed a fast multi-grid approach to solve the BVP performance problems while computing the global potential field. Later, the use of potential distortions through the modification of the partial differential equation were proposed [3], [18] to generate different behaviors other than the traditional greedy approach.

In this paper, we add a local potential distortions slope values in a BVP setup to perform autonomous exploration in uneven 3D terrains.

III. Outdoor exploration using potential fields

A. BVP-Based Exploration

The proposed exploration approach relies on incrementally computing a potential field over a grid map that corresponds to the numerical solution of a Boundary-Value Problem (BVP) [3], [15]. The BVP-based exploration [15] computes a harmonic potential function defined by the Laplace Equation ($\nabla^2 p(x, y) = 0$) together with Dirichlet boundary conditions, i.e., fixed potentials set at the boundaries of the domain (known traversable area). By setting a fixed high potential to obstacles and low potential to unexplored regions, we can generate a potential field, free of local minima, to be used as guide to the exploration process. By following the gradient descent of the potential field, the robot is able to fully explore the environment while developing a smooth trajectory far from obstacles.

However, instead of simply using the original Laplace Equation, it is possible to generate distortions in the potential

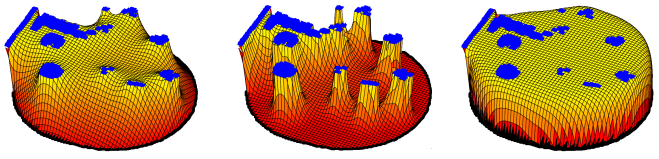

(a) $\epsilon = 0$ (b) $\epsilon = 0.1$ (c) $\epsilon = -0.1$

Fig. 1: Variation in potential field using different global preference values, but same boundary conditions (blue: obstacles, black: goals). With high preferences (b) the potential decreases faster than the original harmonic function (a), while low preferences (c) makes the potential to decrease slower.

field [3] and create regions of different preferences in the environment following Eq. 1,

$$\underbrace{\frac{\partial^2 p(x,y)}{\partial x^2} + \frac{\partial^2 p(x,y)}{\partial y^2}}_{\nabla^2 p(x,y)} - \underbrace{\epsilon(x,y)\left(\left|\frac{\partial p(x,y)}{\partial x}\right| + \left|\frac{\partial p(x,y)}{\partial y}\right|\right)}_{\text{distortion}} = 0, \tag{1}$$

where $\epsilon(x,y)$ is a parameter that indicates the preference of a position (x,y). If $\epsilon(x,y) > 0$, the potential field decreases faster in this position, which makes the potential closer to the goal value, becoming more attractive to the robot. In contrast, if $\epsilon(x,y) < 0$, the position becomes less attractive. Additionally, we are able to change the decay curvature of the potential field by just applying the same distortion globally (in all known environment), as shown in Fig. 1.

Considering that the space is discretized in a grid map, the solution of Eq. 1 is obtained using a finite-difference approximation. The potential of a cell (x,y) (that is not boundary condition) is incrementally updated through a relaxation method as follows,

$$p(x,y) \leftarrow p_h(x,y) - \frac{\epsilon(x,y)}{4} p_d(x,y), \tag{2}$$

where

$$p_h(x,y) \leftarrow \frac{p(x,y+1) + p(x,y-1) + p(x-1,y) + p(x+1,y)}{4}$$

$$p_d(x,y) \leftarrow \left|\frac{p(x,y+1) - p(x,y-1)}{2}\right| + \left|\frac{p(x+1,y) - p(x-1,y)}{2}\right|$$

B. Defining boundary conditions in uneven 3D terrains

The BVP-based exploration requires the definition of two different boundary conditions: obstacles (repulsive potential) and unexplored areas (attractive potential). In this work, we consider a ground robot equipped with two 2D LIDAR sensors: one parallel to ground and other tilted down to detect the ground in front of the robot. For robots like that placed in 2D environments this can be trivial (using only the first LIDAR): cells at the end-points of laser readings are associated to obstacles; cells swept by laser readings before reaching the end-points are associated to free-space; the remaining cells are unexplored. In 3D environments the problem is more difficult, because a range-finder usually captures not only the presence of obstacles, but also the ground curvature, which in general must not be marked as obstacle, otherwise the exploration will never complete.

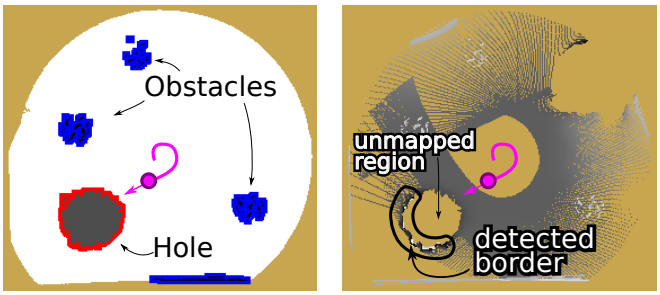

(a) Elevation map (b) Boundary conditions

Fig. 2: Mapping of negative obstacles (hole, in red) is made by detecting cells below the current ground level. Unmapped cells between the detected ones and the robot position are also marked as negative obstacles.

Also, there are "obstacles" that the sensor is not able to directly detect such as slopes, cliffs or holes in the ground.

Many works in outdoor exploration use elevation grids (or variations) to represent the environment and determine its traversability [6], [10], [19]. In the same way, our approach uses a traditional elevation grid that is built as the robot moves, and stores the average of the measured heights of each cell. We analyze the local variation of heights to detect the presence of obstacles and slopes, and classify them as boundary conditions in a 2D grid map M, with cell size s_M, where the potential field will be computed.

Obstacles are detected in two ways:

- By comparing the height $h(x,y)$ of a cell with the average height $\hat{h}(x,y)$ of all neighbor cells inside a kernel of size K_n centered at (x,y). The cell (x,y) is an obstacle if the difference $h(x,y) - \hat{h}(x,y)$ surpasses a threshold h_{obs}.
- When we still do not have enough information about the heights of the neighbors of (x,y), but such cell is being detected by the front-facing sensor and the robot is too close to this cell (closer than a distance d_{obs}).

Holes (or cliffs, slopes) are detected similarly to the work of Joho et al. [19]. When the LIDAR pointing downwards measures the height of a cell, $h(x,y)$, that is sufficiently below the ground level of the robot position, $h(x_r,y_r)$, i.e., when $h(x,y) - h(x_r,y_r) < h_{hole}$, such cell is considered to be a negative obstacle. However, the detected cell usually lies at the bottom of the hole/cliff or in the opposite border, while the nearest border of the hole (in front of the robot) remains unmapped, as shown in Fig. 2. To avoid this issue our approach performs a ray-cast starting from the detected cell and going back to the robot position marking all undetected cells in the way as **negative obstacles**. This technique may mislabel some unknown cells that are near the hole but are not part of it. Luckily, in general this is not a serious problem as it will only make the robot stay farther from the hole.

Lastly, as in the traditional BVP exploration, the **goals** are the cells in unexplored areas, i.e. the ones not measured yet.

C. Using dynamic preferences during exploration

Without disregarding the importance of defining proper boundary conditions in the BVP-based navigation strategy

(otherwise the robot may not be able to perform the full exploration of an environment), one of the main contributions of this method is how to handle local potential distortions using preferences. The application of preferences in previous works [3], [4], [18] was generally made manually over the map or considering simplistic rules, e.g., giving a fixed high preference to cells near obstacles to perform wall-following.

In our work, we propose computing dynamic preferences in all free-space cells as a function of their height values and the height of the current robot position. The idea is to give less preference to regions that are at different heights than the robot, making it to prefer traveling through flatter regions. That is, the algorithm classifies the traversability of the terrain on-the-fly, implicitly defining the safe path the robot should follow using a height-based preference component. Eq. 3 defines the **height-based preference** of a cell (x, y),

$$\epsilon_{height}(x, y) = \max(-\lambda_h \times |h(x_r, y_r) - h(x, y)|, \epsilon_{h_{min}}), \quad (3)$$

as a function of the absolute difference between the height of the cell (x, y) and the robot cell, and a scale factor λ_h. This preference is always negative and limited from some $\epsilon_{h_{min}}$ to 0, where the larger the height difference the more negative the preference is[1]. If the height of a cell is still undefined, $\epsilon_{height}(x, y) = 0$.

Additionally, we propose a global dynamic preference component applied to all cells aiming to alter the decay of the potential field, as exemplified in Fig. 1, and maintain a significant difference of potential around the robot. While preferences are good to guide the robot to regions that are more interesting, there are precautions that should be taken when using them. For instance, if we increase too much the preference of a region, or if the goal is too far from the robot and there are low preference regions between them, the robot may take too long to cross such regions. We can note such situation when the difference of potential field surrounding the robot, $p_{diff}(x_r, y_r)$, becomes too small. $p_{diff}(x_r, y_r)$ is the average of the difference between the potential at the robot position and the potential of neighboring cells inside a kernel of width K_n. This value always stays between 0 and 1, but quickly becomes really small (in the orders of $10^{-6}, 10^{-8}, 10^{-10}$...). In our approach, if $p_{diff}(x_r, y_r)$ becomes smaller than 10^{-10} we momentarily disable the usage of height-based preferences to make the robot reach the goals through the smallest path. Then, only when $p_{diff}(x_r, y_r)$ gets larger than 10^{-4} we reinstate this preference usage.

It is also to deal with this problem of potential flattening that we use a **global preference**[2] as defined in Eq. 4,

$$\epsilon_{global} = \min(-\lambda_g \times \log(p_{diff}(x_r, y_r)), \epsilon_{g_{max}}). \quad (4)$$

The smaller the value of $p_{diff}(x_r, y_r)$, the larger is the value of ϵ_{global}, which is always positive, in contrast to $\epsilon_{height}(x, y)$, that is always negative.

[1]The preference values that can be used are limited to [-2, 2], otherwise the resulting potential in Eq. 2 grows outside [0,1] and the solution diverges.

[2]λ_g is a scale factor and $\epsilon_{g_{max}}$ is the maximum preference value.

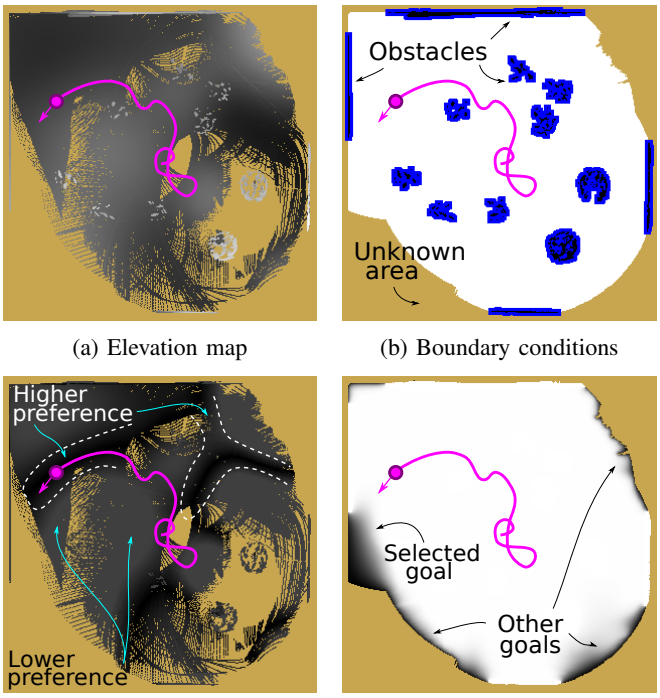

(a) Elevation map (b) Boundary conditions

(c) Preferences map (d) Potential field

Fig. 3: Exploration process prioritizes navigation (robot path, in magenta) towards goals (unexplored area, in dark yellow) over regions with higher preference.

Finally, the **resulting preference** in cell (x, y) is the composition of both types of preferences,

$$\epsilon(x, y) = \epsilon_{global} + \epsilon_{height}(x, y). \quad (5)$$

The value of $\epsilon(x, y)$ is limited to $[\epsilon_{h_{min}}, \epsilon_{g_{max}}]$, given that it is the sum of a positive preference, $\epsilon_{h_{min}} \in [0, \epsilon_{g_{max}}]$, and a negative preference, $\epsilon_{height}(x, y) \in [\epsilon_{h_{min}}, 0]$,

Fig. 3 shows an example of the exploration process using dynamic preferences. The elevation map, (a), is used to generate the boundary conditions, (b), and the height-based preferences, (c), and both are combined to compute the potential field, (d). We can see that there are different goals to be reached in the environment, but the robot chooses the one that can be reached staying in the region of higher preference. Note in (d) that, even though all goals have the same fixed potential value, the selected goal is the most attractive one (the darkest region) due to the effect of the preferences.

IV. Experiments

Our approach was evaluated in simulated experiments using a Pioneer 3-AT robot equipped with two 2D LIDAR sensors (with ranges limited to 12m): one aligned with the robot top plate in parallel to the ground, and one tilted 20° downwards measuring the ground in front of the robot. The experiments were made using ROS and the Gazebo simulator, and considering the parameters defined in Table I. Four scenarios with different characteristics were tested, as shown in Fig. 4: scenario 1 is an almost totally flat terrain containing obstacles and one big slope crossing the environment; scenario 2 is an uneven terrain (as well as

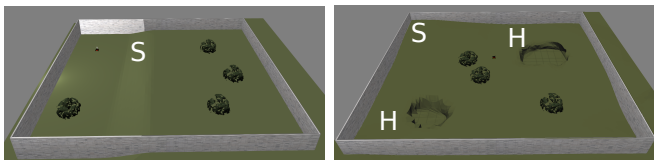

(a) Scenario 1

(b) Scenario 2

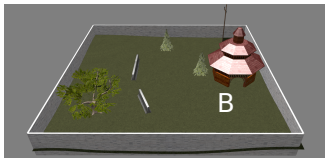

(c) Scenario 3

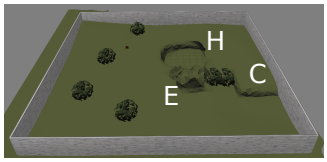

(d) Scenario 4

Fig. 4: Scenarios used in the experiments. *Description:* S - slope; H - hole; B - building; E - elevation/hill; C - cliff.

scenarios 3 and 4) with obstacles, a slope in the corner and two large holes; scenario 3 contains different obstacles and a building with an entrance; scenario 4 contains obstacles, one hole, one steep elevation and one cliff.

Parameter	Value	Definition
s_M	10 cm	Grid cell size
K_n	20 cells	Kernel width
h_{obs}	30 cm	Obstacles height threshold
d_{obs}	1.5 m	Obstacles distance threshold
h_{hole}	-60 cm	Slope height threshold
$\epsilon_{h_{min}}$	-0.5	Min. value of preference
$\epsilon_{g_{max}}$	0.5	Max. value of preference
λ_h	2.0	Scale factor for height preference
λ_g	0.005	Scale factor for global preference

TABLE I: Parameters used in the experiments

Fig. 5 shows the results of experiments in scenario 1, comparing the exploration with and without using preferences. With no preferences, (a), the robot properly classifies obstacles as boundary conditions, but ignores the big slope in the middle of the scenario since it cannot classify it as an obstacle (and it shouldn't). However, disregarding such information may lead the robot to cross the slope region multiple times, which increases the chances of slippage, energy consumption, etc. Using preferences, (b), the robot (if possible) always choose to visit first unexplored regions of higher preference. This leads the robot to fully explore the higher ground, (c), before crossing the slope a single time and completing the exploration (d).

Fig. 6a shows an exploratory path obtained in scenario 2. The robot starts in the middle of the environment (pos. 1) and at the beginning it must avoid the larger hole at the top right corner. The opposite side of the hole is mapped as an obstacle (blue) due to the large height variation detected by the LIDAR in the border of the hole. In turn, the margin at the front of the robot is mapped as negative obstacle (red), due to the absence of height measurements in that region, that prevents the robot from falling. The robot explores the top right corner (pos. 2) but avoids getting too close to it and climbing the slope, based on the preferences. Then it detects and avoids the hole at the bottom left corner (pos. 3), before

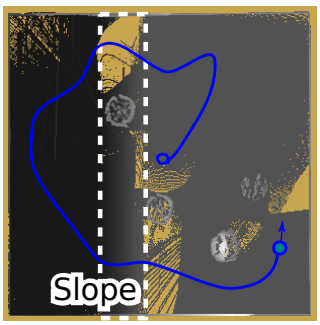

(a) No preferences (final height map)

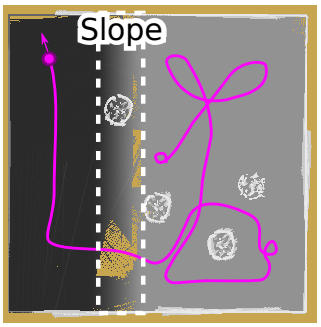

(b) Using preferences (final height map)

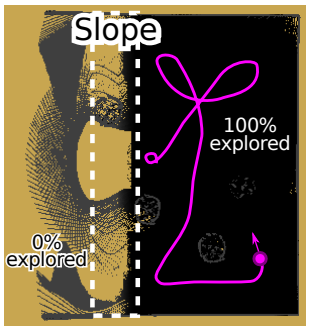

(c) Preferences map at the middle of exploration

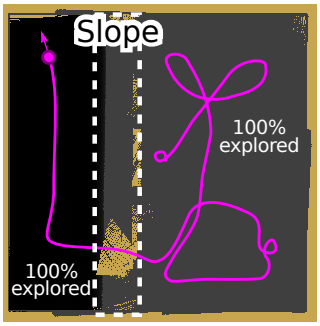

(d) Preferences map at the final of exploration

Fig. 5: Comparison of the exploration process without preferences, (a), and with height-based preferences, (b), in scenario 1. Note the preferences variation in (c) and (d) depending on the robot position (darkest = higher preference).

going to the right side (pos. 4) and finishing the exploration surrounding the first hole (pos. 5).

The exploration in scenario 3 is shown in Fig. 6b. In this scenario, there are obstacles of different types, including a building with an entrance. After mapping part of the environment (pos. 1-3), the robot approaches the entrance of the building (pos. 4). However, the robot does not enter it due to a characteristic of BVP-based exploration. Since it is possible to sense all the building's interior from its door, when the robot reaches such position there is an immediate absence of attractive potentials inside the building, so it turns around and continues the exploration (pos. 5).

Finally, Figs. 6c and 6d show two exploratory trajectories obtained in scenario 4 containing a steep hill, a large hole and a cliff. The interesting aspect is that depending on the path developed by the robot the boundary conditions can be classified differently. In Fig. 6c the robot starts at the top left corner (pos. 1), detects the large hole (pos. 2), then moves towards the bottom right corner (pos. 3). At this position the robot detects the cliff slope from below, just like a barrier, and classify that region as obstacle. Next, the robot proceeds to explore the rest of the environment, and ends visiting the top of the cliff. On the other hand, in Fig. 6d, the robot starts at the top right corner (pos. 1), detects the large hole (from the opposite side of the previous experiment) and moves towards the cliff (pos. 2). Due to the different point of view, the cliff is classified as a negative obstacle given the absence of height measurements in such region. After this, the robot

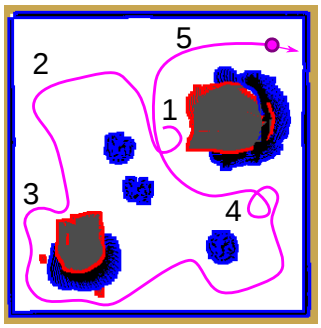

(a) Exploration in scenario 2

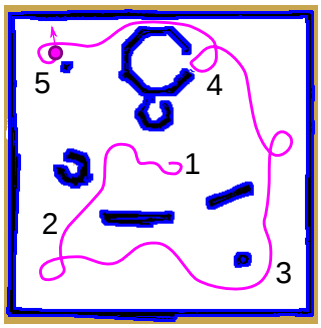

(b) Exploration in scenario 3

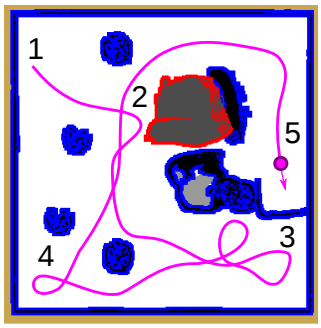

(c) Exploration in scenario 4, starting at the lower ground

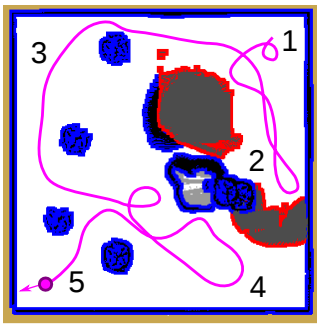

(d) Exploration in scenario 4, starting at the higher ground

Fig. 6: Exploration examples in scenarios 2, 3 and 4 (robot path, in magenta; obstacles in blue; negative obstacles in red).

returns and explores the rest of the environment (pos. 3-5). The main difference that may result from variations in the classification of boundary conditions is the size of the classified region, because in general the classification of obstacles is more accurate than holes. Other than that, both boundary conditions act the same way as repulsive potentials.

V. Conclusion

In this work, we present an exploration strategy using BVP-based potential fields for uneven 3D terrains. The key contributions of this work are: (i) the first potential field strategy to define traversable and untraversable regions on-the-fly using preferences; (ii) a robust strategy to control the effect of distortions of the potential field, with clearly defined parameters; (iii) tests considering different situations and simulation scenarios, which confirm the safety of the approach for real world tests.

The experimental validation has shown that potential fields using BVP is a powerful strategy, that with proper settings of boundary conditions and preferences, is not only able to avoid obstacles and reach goals, but also to make complex decisions during navigation, such as avoiding dangerous areas (e.g. cliffs, holes), avoiding going up and down hills unnecessarily, prioritizing navigation over flat areas, etc.

The present study does not consider the effects of non-holonomic robots with different kinematic constraints – i.e., different robots may climb different slopes depending on robot pose in the terrain, and such parameters are robot dependent. In the future, we plan to address this problem and also consider robots with increased degrees of freedom – e.g., UAVs and AUVs. We are currently testing the algorithm in real world scenarios associated to mine detection robots.

References

[1] S. M. LaValle, *Planning Algorithms*. Cambridge University Press, may 2006.

[2] J. Vallvé and J. Andrade-Cetto, "Potential information fields for mobile robot exploration," *Robotics and Autonomous Systems*, vol. 69, pp. 68–79, 2015.

[3] E. Prestes and P. M. Engel, "Exploration driven by local potential distortions," in *Proc. of IROS*. IEEE, sept. 2011, pp. 1122–1127.

[4] R. Maffei, V. A. M. Jorge, E. Prestes, and M. Kolberg, "Integrated exploration using time-based potential rails," in *Proc. of ICRA*. IEEE, May 2014, pp. 3694–3699.

[5] V. A. M. Jorge, R. Maffei, G. S. Franco, J. Daltrozo, M. Giambastiani, M. Kolberg, and E. Prestes, "Ouroboros: Using potential field in unexplored regions to close loops," in *ICRA*, 2015, pp. 2125–2131.

[6] P. Papadakis, "Terrain traversability analysis methods for unmanned ground vehicles: A survey," *Engineering Applications of Artificial Intelligence*, vol. 26, no. 4, pp. 1373–1385, 2013.

[7] S. Martin and P. Corke, "Long-term exploration amp; tours for energy constrained robots with online proprioceptive traversability estimation," in *Proc. of ICRA*, May 2014, pp. 5778–5785.

[8] I. S. Kweon and T. Kanade, "High-resolution terrain map from multiple sensor data," *IEEE Transactions on Pattern Analysis and Machine Intelligence*, vol. 14, no. 2, pp. 278–292, Feb 1992.

[9] S. Kuthirummal, A. Das, and S. Samarasekera, "A graph traversal based algorithm for obstacle detection using lidar or stereo," in *Proc. of IROS*, Sep. 2011, pp. 3874–3880.

[10] B. Suger, B. Steder, and W. Burgard, "Traversability analysis for mobile robots in outdoor environments: A semi-supervised learning approach based on 3d-lidar data," in *ICRA*, 2015, pp. 3941–3946.

[11] À. Santamaria-Navarro, E. H. Teniente, M. Morta, and J. Andrade-Cetto, "Terrain classification in complex three-dimensional outdoor environments," *J. of Field Robotics*, vol. 32, no. 1, pp. 42–60, 2015.

[12] L. Yoder and S. Scherer, "Autonomous exploration for infrastructure modeling with a micro aerial vehicle," *Field and service robotics*, pp. 427–440, 2016.

[13] R. T. Rodrigues, M. Basiri, A. P. Aguiar, and P. Miraldo, "Low-level active visual navigation: Increasing robustness of vision-based localization using potential fields," *IEEE Robotics and Automation Letters*, vol. 3, no. 3, pp. 2079–2086, July 2018.

[14] S. Shen, N. Michael, and V. Kumar, "Stochastic differential equation-based exploration algorithm for autonomous indoor 3d exploration with a micro-aerial vehicle," *The International Journal of Robotics Research*, vol. 31, no. 12, pp. 1431–1444, 2012.

[15] E. Prestes, P. M. Engel, M. Trevisan, and M. A. P. Idiart, "Exploration method using harmonic functions," *Robotics and Autonomous Systems*, vol. 40, no. 1, pp. 25–42, 2002.

[16] E. Prestes, M. Trevisan, M. A. P. Idiart, and P. M. Engel, "Bvp-exploration: further improvements," in *IROS*, 2003, pp. 3239–3244.

[17] R. Silveira, E. Prestes, and L. Nedel, "Fast path planning using multi-resolution boundary value problems," in *Proc. of IROS*. IEEE, oct. 2010, pp. 4710–4715.

[18] E. Prestes and M. Idiart, "Sculpting potential fields in the bvp path planner," in *Proc. of ROBIO*, dec. 2009, pp. 183–188.

[19] D. Joho, C. Stachniss, P. Pfaff, and W. Burgard, "Autonomous exploration for 3d map learning," in *Autonome Mobile Systeme*. Springer, 2007, pp. 22–28.

[20] A. Bircher, M. Kamel, K. Alexis, H. Oleynikova, and R. Siegwart, "Receding horizon path planning for 3d exploration and surface inspection," *Autonomous Robots*, vol. 42, no. 2, pp. 291–306, 2018.

[21] P. Vlantis, C. Vrohidis, C. P. Bechlioulis, and K. J. Kyriakopoulos, "Robot navigation in complex workspaces using harmonic maps," in *Proc. of ICRA*. IEEE, 2018, pp. 1726–1731.

[22] J.-M. Muñoz, E. Muñoz-Panduro, and O. E. Ramos, "Autonomous motion of a mobile robot based on potential fields and polar control," in *Proc. of INTERCON*. IEEE, 2018, pp. 1–4.

[23] P. Friudenberg and S. Koziol, "Mobile robot rendezvous using potential fields combined with parallel navigation," *IEEE Access*, vol. 6, pp. 16 948–16 957, 2018.

[24] J. Chen, P. Kim, Y. K. Cho, and J. Ueda, "Object-sensitive potential fields for mobile robot navigation and mapping in indoor environments," in *Proc. of UR*. IEEE, 2018, pp. 328–333.